IOSR Journal of Nursing and Health Science (IOSR-JNHS)
e-ISSN: 2320–1959.p- ISSN: 2320–1940 Volume 14, Issue 2 Ser. 5 (Mar. – Apr. 2025), PP 07-18
www.iosrjournals.org

"Deep Learning-Based Mr-Only Dose Estimation For Adaptive Radiation Therapy"

Syed Anam Parvez, Ishant, Deepak Katiyar
Teerthanker Mahaveer University, Moradabad, Uttar Pradesh, [244001]

Abstract:
This research explores the feasibility of employing a novel distance-based representation of 3D CT-scan images to train deep learning models for predicting radiation dose distribution in treatment planning. The proposed approach is designed to enhance the generalizability of deep learning models by incorporating domain knowledge into the representation method. Traditional knowledge-based planning techniques rely on manually extracted features from 3D CT scans and patient-specific attributes to estimate optimal dose distribution for cancerous regions and surrounding organs at risk. While recent advancements have demonstrated improved accuracy in voxel-level dose prediction using deep learning, the limited availability of training data has led most studies to adopt 2D contour-based anatomical representations. However, these methods often lose critical volumetric information and are highly sensitive to variations in patient positioning and orientation. The distance-based representation introduced in this study overcomes these limitations by preserving volumetric distance data while maintaining the practicality of 2D slice-based imaging. Prior research in radiation therapy planning suggests a strong correlation between the proximity of organs at risk to the cancerous region and their susceptibility to excessive radiation exposure. Instead of relying on conventional contour-based features, the proposed approach replaces contour values with voxel-wise distance measurements from the tumor. This adaptation enhances robustness against shifts in patient positioning during imaging and planning. To evaluate the effectiveness of this approach, deep learning models utilizing distance-based representations were applied to prostate cancer cases. Experiments included predictions of patient vulnerability and voxel-level dose distributions using convolutional neural networks and U-Net architectures. The results were benchmarked against contour-based U-Net models and conventional machine learning techniques employing engineered features. Findings indicate that the proposed method achieves performance comparable to or exceeding existing state-of-the-art models for prostate cancer dose distribution prediction.

Keywords: *Deep learning, knowledge-based planning (KBP), intensity-modulated radiation therapy (IMRT), Deep Learning, Dose Distribution, 3D Distance Matrices, CT-Scan, Segmentation, Inter-patient Variability, Anatomical Structures, Target Volumes, Spatial Relationships, Predictive Accuracy ETC.*

Date of Submission: 05-04-2025 Date of Acceptance: 15-04-2025

I. Introduction:

Radiation therapy is a widely used and effective method for treating prostate cancer, aiming to eliminate or control the growth of cancerous cells. However, the treatment's success depends on accurately directing and controlling the radiation dose. If the radiation dose is insufficient, the tumor may not be effectively eradicated, increasing the likelihood of recurrence. On the other hand, excessive radiation exposure can damage surrounding healthy tissues, raising the risk of complications or secondary malignancies. Despite careful treatment planning, variations in patient anatomy and tumor geometry can make some individuals more vulnerable to receiving unintended doses. Therefore, early assessment of a patient's susceptibility and precise dose distribution predictions are essential for optimizing treatment strategies.[1] Approximately two-thirds of all cancer patients undergo Radiation Therapy either as a standalone treatment or in combination with other medical interventions. Among the significant advancements in External Beam Radiation Therapy (EBRT) is the development of Intensity-Modulated Radiation Therapy (IMRT), which leverages variable beam intensities to target malignancies more precisely. IMRT offers enhanced dose delivery to the planning target volume (PTV) while reducing exposure to surrounding organs at risk (OARs), surpassing the capabilities of traditional 3D conformal radiation therapy. However, IMRT's treatment planning remains a complex and time-intensive task.[4] The planning workflow involves two iterative stages. Initially, the treatment planner adjusts dose-volume constraints and other key parameters to optimize dose distribution—maximizing the dose to the PTV while minimizing impact on critical structures. This process is often conducted through a trial-and-error method, requiring significant time and effort. Subsequently, the physician evaluates the preliminary plan and provides feedback, initiating another round of refinement. This cycle repeats until a satisfactory plan is approved, with the timeline ranging from several hours

to over a week, depending on the complexity of the treatment site.[6] To address the inefficiencies of this traditional planning process, researchers have explored various mathematical optimization techniques. Multicriteria optimization enables the generation of several treatment plans that reflect different tradeoffs between OAR sparing and PTV coverage, offering clinicians more flexibility in decision-making. Beam orientation optimization aims to identify ideal beam directions, improving on manually determined configurations. Additionally, direct aperture optimization, or machine parameter optimization, focuses on determining optimal beam shapes and intensities to ensure deliverable and high-quality treatment plans.[25] Commercial treatment planning software such as Eclipse (Varian Medical Systems), Pinnacle (Philips Radiation Oncology), and RayPlan (RaySearch Laboratories) incorporate these optimization methods. Despite their advantages, these platforms still demand extensive manual input—adjusting structure weights, beam geometry, and dose-volume constraints—resulting in planning variability across users. Such reliance on individual expertise can lead to inconsistent and potentially suboptimal plans.[26] In response, knowledge-based planning (KBP) approaches have emerged to streamline and improve the planning process. KBP systems utilize prior high-quality treatment plans to guide the development of new plans. One prominent example is RapidPlan by Varian Medical Systems, which predicts dose-volume histograms (DVHs) based on patient-specific anatomical features. Studies have shown that RapidPlan can generate clinically acceptable plans more efficiently than conventional planning methods in many cases. However, the system still requires manual adjustments for complex cases and is constrained by the limited size and scope of its training datasets. Additionally, traditional KBP models often depend on predefined features and struggle to generalize beyond their training data. Recent advancements in deep learning have provided new opportunities to automate and enhance IMRT planning. Unlike earlier machine learning methods, deep learning techniques automatically extract features from data, eliminating the need for manual feature engineering. The advent of fully convolutional networks (FCNs) introduced voxel-wise dose prediction capabilities, enabling the generation of DVHs directly from anatomical inputs. Several studies have since applied deep learning models to predict dose distributions for IMRT and Volumetric Modulated Arc Therapy (VMAT) in various cancer types, including lung, prostate, and head-and-neck cancers. However, most models employed static beam configurations, limiting their flexibility in clinical practice.[1] One notable development involved a model that accounted for variable beam angles in lung IMRT dose prediction. Nevertheless, deep learning models typically produce a single dose distribution per patient, whereas Pareto optimal models can generate multiple plans representing different tradeoffs among critical structures. Some studies have demonstrated that deep learning models can predict such Pareto optimal plans using anatomical information and fixed beam setups. This study proposes a novel approach to predict Pareto optimal dose distributions for prostate IMRT using deep learning networks that incorporate both anatomical structures and variable beam configurations. A key innovation of this work is the integration of beam orientation flexibility into the dose prediction model. This enables planners to rapidly explore different beam arrangements, including those beyond conventional clinical protocols.[37] Two deep learning models are developed and compared. The first model (Model I) incorporates beam angles as a binary vector input, while the second model (Model II) represents beam setup information using a conformal dose distribution generated from the same beam angles. Model II serves as a benchmark and aligns with previously established methods, such as the one introduced by Ana et al., which relied on the fluence-convolution broad beam method for dose calculation. In this study, a simpler algorithm is employed to create beams conformal to the PTV. Overall, this work empowers treatment planners by providing a deep learning-based framework that facilitates real-time adjustment of PTV and OAR tradeoffs, beam quantity, and beam geometry—enhancing both the speed and quality of IMRT planning for prostate cancer.[15] A widely used approach for evaluating normal tissue vulnerability is the Normal Tissue Complication Probability (NTCP) model. This model utilizes dosimetric features, such as dose-volume histograms (DVHs), to estimate the likelihood of radiation-induced complications in healthy tissues. The Quantitative Analysis of Normal Tissue Effects in the Clinic (QUANTEC) initiative has highlighted the potential of machine learning techniques to enhance predictive accuracy. Traditional predictive models rely on engineered anatomical features to account for variations in organ-at-risk (OAR) exposure across different patients. Recent advancements have demonstrated that deep learning models can achieve superior performance by learning features directly from 3D CT scan images. However, due to the limited availability of training data, most studies preprocess the scans by extracting contours and representing patient anatomy using 2D slices. While this method simplifies the learning process, it fails to preserve crucial spatial information, such as the three-dimensional positioning and orientation of organs relative to the tumor. Although deep learning models employ augmentation techniques to address variations in patient positioning, these adjustments may not be sufficient in real clinical scenarios.[19] This study introduces a novel distance-based representation that emphasizes the 3D spatial relationships between OARs and the planning target volume (PTV). Unlike conventional contour-based methods, this approach retains volumetric information even when images are processed in 2D slices. The proposed framework is designed to enhance the accuracy and robustness of knowledge-based dose prediction models. Comparative analyses between the distance-based approach and previously established contour-based and hand-crafted feature models indicate that the new representation

performs comparably or better. The motivation for replacing conventional image and contour-based representations with a distance-based approach lies in its ability to improve model generalization. By making dose predictions less sensitive to variations in patient positioning, this method enhances the potential for transferring knowledge across different patients and treatment institutions, ultimately improving radiation therapy planning.

Technical Significance:

This study evaluates the effectiveness of a distance-based representation within deep learning frameworks for predicting dose distribution in radiation treatment planning. The proposed approach integrates established domain knowledge from radiation therapy with advanced deep learning techniques. A key challenge in deep learning applications is the limited availability of labeled data, which can hinder the generalizability of predictive models. Our work aligns with the perspective that incorporating prior domain knowledge can enhance model reliability and mitigate generalization issues, particularly when access to extensive training datasets is constrained.[37]

Clinical Relevance:

Radiation therapy is a widely utilized and effective treatment approach for cancer management. However, the planning process remains a complex and iterative task that requires manual input from physicians and medical planners. One of the key challenges is that the ideal dose distribution may not always be feasible due to patient-specific anatomical variations, tumor geometry, and other clinical constraints. As a result, it is crucial to provide physicians with insights into what dose distribution is realistically achievable for each individual patient or to identify cases where clinical criteria may not be met.[39] This study aims to address these challenges by offering an early assessment of patient vulnerability based on anatomical limitations (Task 1). Additionally, it provides an estimation of the optimal dose distribution using organ-specific features and prior knowledge from similar patient cases (Task 2). The structure of this paper is organized as follows: Section II outlines the motivation for the proposed distance-based representation and the methodology for data extraction. Section III details the learning framework and model development process. In Section IV, we present an in-depth evaluation of the approach along with a discussion of the assessment results. Lastly, Section V explores the potential implications of this research and possible future directions.[41]

II. Dataset: Distance-Based Representation:

Representation Motivation:

Importance Of Organ-To-Target Distance In Treatment Planning:

The spatial relationship between an organ and the target treatment volume is a critical anatomical factor in radiation therapy planning. When a healthy organ is located close to the cancerous region, it becomes more susceptible to receiving unintended high radiation doses. To quantitatively assess this relationship, earlier research proposed metrics such as the Distance-to-Target Histogram (DTH) and the Overlap Volume Histogram (OVH). These tools help in evaluating how organ proximity influences dose distribution during therapy.[22]

Figure 1: Conformal Dose Corresponding To Different Beam Angles (1-10)

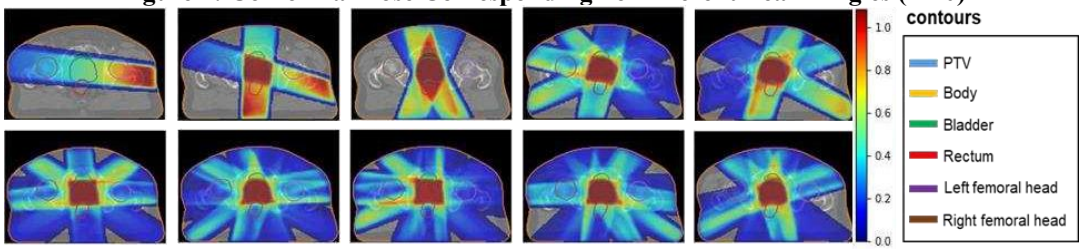

Building on this, highlighted several key measures that significantly impact the prediction of variability in Dose-Volume Histograms (DVH) across different patients. These include:

- The median distance between the Organ-at-Risk (OAR) and the Planning Target Volume (PTV).
- The percentage of the OAR volume located within a defined distance from the PTV.
- The fraction of the OAR that overlaps with the PTV.
- The proportion of the OAR volume situated outside the primary radiation field.

Deep learning models have shown remarkable effectiveness in recognizing and learning local shape-related features, which has encouraged researchers to explore their potential in capturing inter-patient variability in radiation dose distribution. Motivated by previous findings, we propose using three-dimensional distance matrices—derived from segmented 3D CT scan images—as a novel input representation for deep learning

frameworks. This approach builds upon earlier studies that highlighted the significance of spatial relationships between anatomical structures and target volumes, aiming to enhance the predictive accuracy and generalizability of dose distribution models.[27]

Data Extraction:

This study utilizes data from 216 patients diagnosed with prostate cancer who underwent radiation therapy. Prostate cancer was specifically chosen due to the close proximity of two critical organs—bladder and rectum—to the prostate, which serves as the treatment target. When these adjacent organs receive excessive radiation, patients may experience significant side effects. Therefore, being able to predict the radiation dose these organs might absorb based on their anatomical positioning is vital for refining treatment plans and minimizing risks. The initial dataset includes 3D contour data of anatomical structures, 3D dose distributions, and the prescribed radiation doses. To tailor the dataset for our study, several preprocessing steps were performed. First, 3D dose matrices specific to the bladder and rectum were generated using their respective contour data and planned dose distributions. Any dose information not associated with these two organs was excluded.[14] Cumulative Dose-Volume Histograms (DVHs) were computed using dose intervals of 50 cGy. For each organ, the DVH reflects the percentage of the organ's volume receiving at least a certain dose, with all dose values normalized according to each patient's prescribed dose.[19] To represent spatial relationships, 3D distance matrices were generated from the contoured CT scans. These matrices—referred to as distance3d in this study—are unique to each patient's organ-at-risk (OAR), either the bladder or rectum. Each voxel within the matrix holds the shortest distance from that voxel to the surface of the planning target volume (PTV), which is the prostate in this case. Voxels located outside the organ are assigned a value of zero, while those overlapping with the PTV receive negative values to indicate shared space. Additionally, values for voxels outside the radiation field were adjusted to account for "out-of-field" conditions described in earlier research.

III. Methodology Deep Learning:

Traditional knowledge-based planning techniques rely on handcrafted features extracted from 3D CT scans to estimate the optimal radiation dose for both the tumor and nearby critical organs. However, recent advancements in medical imaging have shown that deep learning-based features often outperform manually engineered ones in terms of predictive accuracy. Despite these advantages, a significant challenge remains—deep learning models require large volumes of labeled data, which are often limited in the field of radiation treatment planning. This limitation raises concerns about the generalizability of such models when applied across diverse patient populations.[21]

Model I:

The architecture of Model I, as illustrated in Figure 2, processes three input channels: one each for the planning target volume (PTV), the body, and the organs-at-risk (OARs). Rather than using binary masks alone, each voxel within a structure is weighted using the corresponding structure weights, , as defined in Equation 3. Voxels within a structure are assigned a value of , while all other voxels are set to zero. The PTV and body channels contain only their respective structure data, whereas the OARs channel consolidates data from the bladder, rectum, femoral heads, and tuning structures.[19] As outlined in Section 2.1, all imaging data were resampled to a voxel size of 5 mm^3. To ensure consistency across patient datasets, all input volumes were standardized into a fixed array size of $96 \times 96 \times 32$. The body segmentations span the CT image slices. Because the weights range from 0 to 1, the anatomical inputs also fall within this normalized range. In addition to anatomical data, Model I incorporates a second input: a Boolean vector of length 180 representing beam angles at 2-degree intervals. Angles selected for beam delivery are marked as 1, and the remaining are marked as 0. This vector is processed through a fully connected layer with an output dimension of 2304. The output is then reshaped into a 4D tensor of size (6, 6, 2, 32), aligning with the spatial dimensions of the downsampled features within the network. This reshaped tensor is concatenated along the channel axis with the image features to enable further joint learning.[13]

Model II:

Model II maintains the same core architecture as shown in Figure 2 but omits the beam angle vector input used in Model I. Instead, it accepts a four-channel input: the first three channels are identical to those in Model I (PTV, body, and OARs), while the fourth channel includes the conformal dose distribution corresponding to a specific beam configuration, as discussed in Section 2.2.

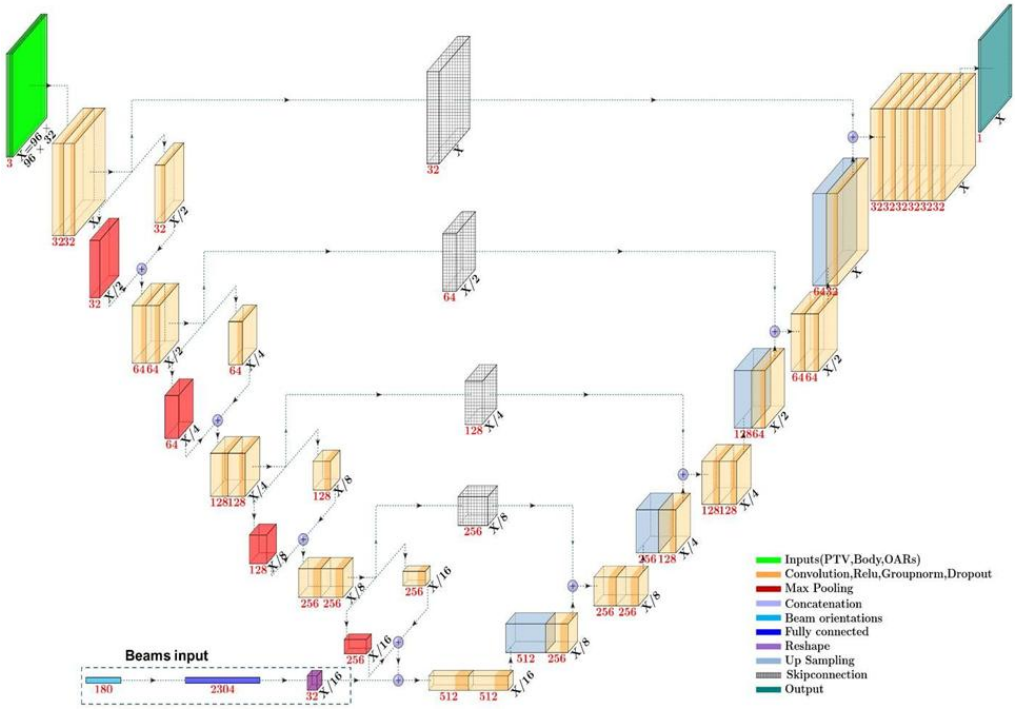

Figure 2: Deep Learning Models Used In The Study.

Like Model I, each input channel has dimensions of 96 × 96 × 32, with anatomical values normalized between 0 and 1. The conformal dose channel is also normalized by dividing each voxel by the maximum dose in the volume, ensuring its range is also between 0 and 1.[19] To address this issue, several strategies have been widely adopted in medical image analysis. These include dimensionality reduction, transfer learning, and the use of deep residual networks such as U-Net to enhance model efficiency even with smaller datasets. In our study, we incorporated these techniques into the design of our learning model to assess the effectiveness of the proposed distance-based representation. The upcoming sections provide a detailed explanation of each method and its role in our experimental setup.

Dimensionality Reduction And Representation Strategy:

Reducing 3D data to 2D formats is a common approach to decrease the number of input variables, thus lowering the demand for large datasets during model training. However, this process often comes with the drawback of information loss. In our approach, we mitigate this issue by preserving key spatial relationships through the use of distance3d matrices, which maintain the essential three-dimensional distance information. Additionally, the slicing technique employed retains critical structural and local features, minimizing the impact of dimensionality reduction. While statistical methods such as Principal Component Analysis (PCA) are traditionally used for dimensionality reduction due to their ability to preserve the most variance in data, these techniques are generally optimized for global patterns. As a result, they may discard the local spatial details that are crucial for feature extraction in deep learning applications. To maintain these local patterns, we chose not to apply such methods.[3] Instead, we focused on anatomical slicing along three standard body planes: sagittal (left to right), coronal (front to back), and axial (top to bottom). These slices reflect real-world clinical imaging practices and preserve interpretability. For prostate cancer CT scans, axial slicing is typically used, indexing from the head toward the feet. In our initial experiments (Task 1), we explored the effectiveness of each slicing direction.[19] Since our proposed representation is rooted in 3D spatial distances, it inherently retains more volumetric information compared to conventional 2D representations. This was validated by observing improved model performance when using 3D distance matrices in comparison with their 2D counterparts in the same experimental conditions (Task 1). After performing the slicing, each 2D image slice is treated as an individual training sample. This not only increases the number of training examples but also enhances the network's resilience to slice positioning variations. It's important to note that slices consisting entirely of zero values—indicating the absence of any relevant anatomical structure—do not contribute useful information. These were therefore excluded from the classification phase in Task 1.[12]

Transfer Learning: VGG-16:

In most machine learning tasks, it is generally assumed that the training and testing datasets are drawn from the same distribution. Transfer learning, however, challenges this assumption by enabling models trained on one dataset or task to be adapted to another, often with a different data distribution. This technique has gained popularity, particularly in deep learning, due to its ability to leverage existing models and reduce the need for extensive labeled data — a common challenge in specialized domains like medical imaging.[13] In this study, we applied transfer learning to evaluate how effectively the proposed distance-based representation could benefit from pre-trained models developed on general (non-medical) image datasets, helping to address the limited availability of annotated medical data (Task 1). Since distance matrices resemble grayscale images—where pixel values represent depth-like information relative to the Planning Target Volume (PTV)—they can be used as input to models designed for image processing.[11] Motivated by the work of Tran et al. [15], we adopted the VGG-16 architecture [14], a well-established convolutional neural network originally designed for image classification tasks in the ImageNet competition. VGG-16 consists of 16 layers, including five convolutional blocks followed by three fully connected layers. Its layered structure supports the progression of data from capturing low-level visual features to high-level abstractions. To utilize VGG-16 in our experiments, we retained the first four convolutional blocks with their pre-trained weights frozen to preserve the generic image features they capture. The output from the final convolutional block served as encoded features, which were then passed through a series of fully connected layers trained specifically to classify patients based on their susceptibility to receiving higher doses in organs at risk (OARs). Because VGG-16 expects RGB image input, we replicated the single-channel distance matrix into three channels, effectively mimicking the required format while maintaining the depth-related information relevant to our task. A schematic of the adapted CNN architecture is illustrated in Figure 1.

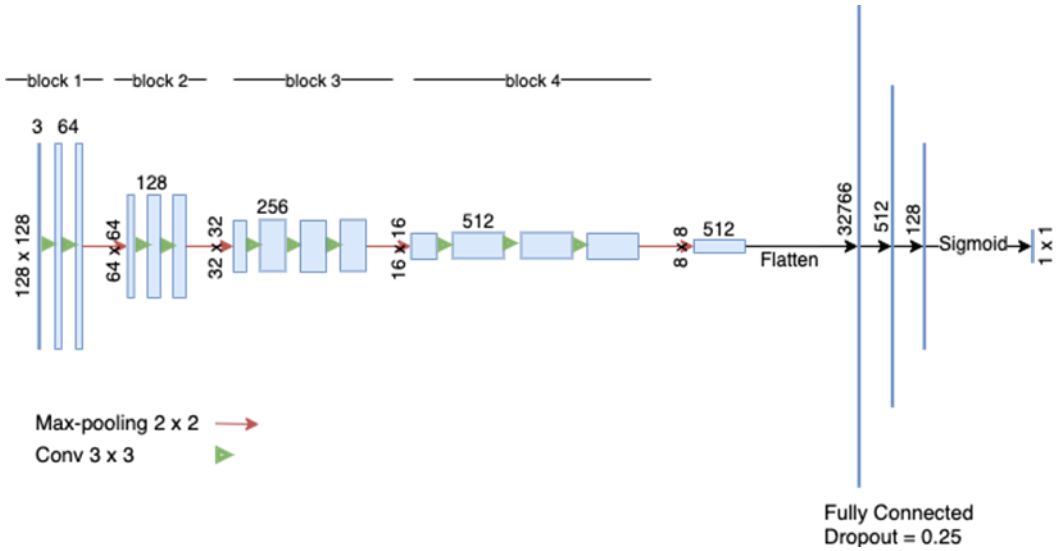

Figure 3: These Are Followed By Three Fully Connected Layers Utilizing Relu Activation Functions, And A Final Sigmoid Layer Designed For Binary Classification.

U-Net Architecture For Dose Prediction:

U-Net is a well-known architecture from the fully convolutional network (FCN) family, originally introduced for medical image segmentation tasks [12]. Its design, which eliminates fully connected layers and incorporates skip connections between the encoder and decoder paths, enables efficient learning even when training data is limited. These skip connections help retain spatial context and improve the quality of segmentation. In recent studies [4], [9]–[11], U-Net-based models have been effectively employed to predict voxel-wise radiation dose distributions using anatomical contour information. In this study, we adopted a U-Net structure closely aligned with the original design [12], adapting it to our specific task. To evaluate the effectiveness of our proposed distance-based input representation, we implemented the U-Net model and compared its performance to that of models using conventional contour-based inputs. The architectural overview of our model used for prediction is illustrated in Figure 2.

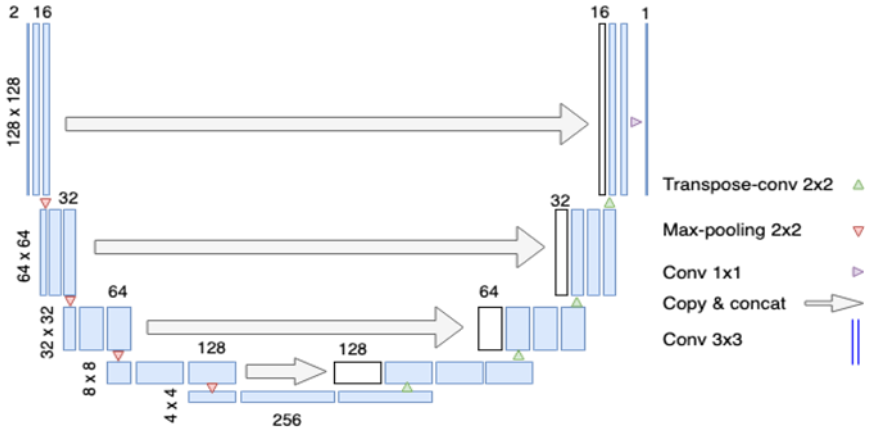

Figure 4: The Implemented U-Net Model Processes A Two-Channel 128 × 128 Distance. A Single Output Channel Is Used To Represent The Predicted Dose.

IV. Evaluation And Result: Dose Prediction:

The effectiveness of the distance-based representation is tested through two predictive experiments. The first task, detailed in Section IV-A, involves classifying patients based on how susceptible their organs-at-risk (OARs) are to receiving high radiation doses. For this, a pre-trained convolutional neural network (CNN) is utilized. The objective is to determine whether a significant feature—namely vulnerability—can be inferred directly from the anatomical structure of each OAR, evaluated independently.[19] This approach is built on the premise that the proposed representation retains sufficient anatomical and spatial information from CT images, making it possible for models trained on general visual data to extract meaningful patterns. Additionally, it suggests that relevant characteristics of individual organs can be effectively analyzed without necessarily considering the full anatomical context.[41]

Task 1: Predicting Vulnerability Of Organs-At-Risk:

As introduced earlier, one of the goals in creating a high-quality radiation therapy plan is to minimize the dose received by surrounding healthy tissues, also known as organs-at-risk (OARs). However, due to anatomical differences, some patients may be inherently more susceptible to higher radiation exposure. This task aims to identify those patients by predicting their vulnerability. This is structured as a binary classification problem, where the model distinguishes between more and less vulnerable patients based on 2D slices from the 3D distance matrices (referred to as *distance3d*). For this purpose, we use the VGG-16 model with pre-trained weights, as described in Section III-B.[11] The original dataset comprises distance matrices of the bladder and rectum from 216 prostate cancer patients. Each matrix includes 300 slices, with each slice sized at 192 × 252 pixels. To create input for the classification task, we extract five non-zero consecutive 2D slices from the middle region of each 3D matrix. This is done across three anatomical views—sagittal, coronal, and axial—which increases the sample size fivefold and simplifies the learning task, albeit with some loss of information. For the second task—voxel-wise dose prediction—we designed multiple experiments to allow comparison with prior studies ([11], [18]). The number of slices used in training and validation for these experiments varies and is specified in the relevant sections. For clarity, we use the variables *st* and *sv* to indicate the number of selected slices for training and validation, respectively.

Task 2: Predicting Voxel-Level Dose Distribution:

The second predictive task (outlined in Section IV-B) involves estimating the voxel-level radiation dose distribution using training data from high-quality treatment plans of previous patients. For this, we utilized a U-Net architecture, which has been widely adopted in recent studies for dose prediction at the voxel level using deep learning techniques.[11] To prepare the data for this task, the original 3D matrices were converted into 2D slices, as discussed earlier in Section III-A. Each slice was then center-cropped to a standardized size of 128 × 128 pixels. Table I presents both the original dimensions of the distance matrices for each organ-at-risk (OAR) and the final dataset size after preprocessing. The contour matrices follow a similar format to the distance matrices but contain binary values—voxels within the OAR are labeled as one, and those outside are labeled as zero. The preprocessing steps (cropping and slicing) were consistently applied to the distance, contour, and dose matrices to ensure alignment across all data types. For the prediction task, each data sample is formed by combining bladder and rectum slices as separate input channels. Importantly, data splitting into training, validation, and testing sets is done at the patient level to prevent data leakage. All slicing and related processing are performed only after this

division. A visual summary of the experimental workflow is provided in Figure 3. Details about the computational environment, including hardware and software configurations, are listed in Tables II and III.

Table I: Dimension Of The Input Features:

Class	Test	Input
Original Dataset	-	2 * (216, 300, 192, 252, 1
Classification Task	Test	2 * (180, 128, 128, 3)
Dose Prediction Task	Train	St * (2, 172, 128, 128, 1)
Dose Prediction Task	Validation	Sv * (2, 44, 128, 128, 1)

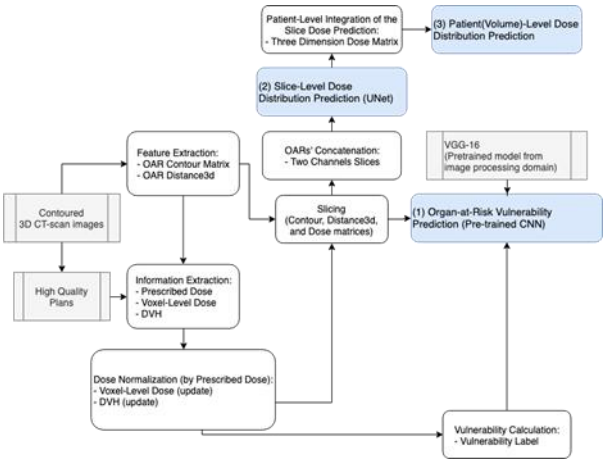

Figure 5: This Diagram Presents A Comprehensive Overview Of The Data Sources, Processing Steps, And Prediction Outcomes Involved In The Study.

Table II: Specification Software - Dose Prediction Task:

S.N	System	Range
1	Operating System	Debian 9
2	Programming Language	Python 3.6.4
3	Deep Learning Back-End	Pytorch 1.1.0

Table III: Specification Of The Experiments' Setting:

S.N	Parameter	Cnn Setting	U-Net Setting
1	Optimizer	Adam	Adam
2	Loss Function	Binary Crossentropy	Mean Squared Error
3	Abstraction (Downsampling)	4	4
4	Epochs	100	200
5	Batch Size	32	16
6	Learning Rate	0.000001	0.0001

In this study, vulnerability labels are used as the target output for the machine learning model. To maintain a balanced label distribution, each patient is compared against an average case. The metric chosen for prediction is the *dose-at-50*, although this model can be adapted to predict doses at other volume thresholds as well.[45] The *dose-at-50* refers to the maximum radiation dose received by at least 50% of an organ, based on high-quality radiotherapy plans. These dose values are normalized by dividing by the prescribed dose, allowing for fair comparisons across all patients. Each patient's dose ratio is then compared to the population mean: if a patient's normalized dose is equal to or greater than the mean, they are considered more vulnerable (assigned a label of 1); otherwise, they are labeled as less vulnerable (label 0). It's important to note that vulnerability labeling is specific to each organ-at-risk (OAR). A patient's vulnerability in the bladder, for instance, does not imply the same status in the rectum. While correlations may exist, each OAR—specifically the bladder and rectum in this study—is independently labeled and analyzed. The dataset comprises information from 216 patients and the entire analysis is conducted on a cloud-based virtual machine. Details regarding experimental setup, framework specifications, and data characteristics are provided in Tables I, II, and III. For model evaluation, a five-fold cross-validation approach is used. In each fold, 173 patients form the training set, and 43 are used for testing. Although slices of medical images are treated as separate data points, all slices from a single patient are consistently assigned to either the training or testing set, avoiding any data leakage.[43]

Standard binary classification metrics—accuracy, precision, recall, and F1-score—are used for performance evaluation. The results, as summarized in Table IV, show an average accuracy of **84.89%** for predicting bladder vulnerability and **60.34%** for the rectum. Given the observed distribution in Figure 4 and the proximity of

some cases to the decision boundary, the bladder prediction performance is particularly promising. These findings motivate further investigation into the prediction of full dose distribution matrices

Table IV: The Table Presents The Average Performance Metrics Obtained Through Five-Fold Cross-Validation. For Each Fold, The Model Was Trained On 720 Data.

S.N	Organ-at-Risk (OAR)	Slicing Plane	Precision (%)	Recall (%)	F-score (%)	Accuracy (%)
Validation Results						
1	Bladder	Axial	80.02 ± 8.11	82.89 ± 1.89	78.90 ± 4.21	82.67 ± 2.47
2		Coronal	82.61 ± 10.63	77.67 ± 1.99	77.24 ± 6.12	80.11 ± 4.80
3		Sagittal	80.51 ± 7.66	82.42 ± 5.74	79.44 ± 6.06	81.44 ± 5.89
4	Rectum	Axial	55.27 ± 15.81	49.94 ± 11.23	48.35 ± 9.38	51.33 ± 5.78
5		Coronal	63.27±12.42	63.27 ± 10.99	59.64 ± 6.64	63.44 ± 3.05
6		Sagittal	65.82 ± 14.83	66.13 ± 9.03	63.07 ± 8.66	66.67 ± 1.96
Test Results						
1	Bladder	Axial	79.14 ± 2.77	81.16 (±5.32)	78.55 (±3.28)	77.89 (±3.36)
2		Coronal	83.10 ± 3.74	92.45 (±3.00)	86.08 (±2.66)	84.89 (±3.13)
3		Sagittal	75.22 ± 3.05	85.19 (±2.29)	77.89 (±3.25)	75.33 (±3.38)
4	Rectum	Axial	57.34 ± 1.69	44.81 (±12.98)	48.39 (±7.77)	51.33 (±1.71)
5		Coronal	50.46 ± 0.93	46.79 (±6.17)	47.64 (±3.61)	48.56 (±2.45)
6		Sagittal	60.48 ± 6.58	60.61 (±3.90)	58.43 (±2.51)	60.34 (±4.48)

V. Evaluation Of Dose Distribution Using 3d Volumetric Data:

To enable a comprehensive patient-level analysis, predictions were carried out across all slices within each patient's 3D volume. The model was trained using 10 strategically selected slices per patient from the distance3d set, ensuring that the data distribution remained balanced and not overly influenced by denser regions. Given the prevalence of zero-intensity slices, a probabilistic sampling approach was employed—this method favors slices with a higher count of non-zero voxels, thereby enhancing the representativeness of the training data. For evaluation, the model's performance was assessed on the entire volume of each patient in the validation set, allowing for a detailed calculation of dose distribution across three dimensions. Training and validation losses were monitored throughout the process.

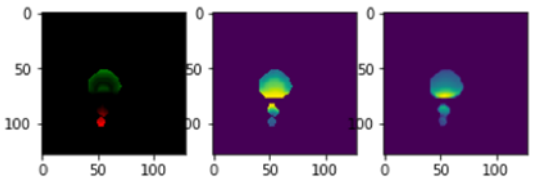

(A)Distance Matrix (Input), Dose Distribution (Expected Output), And Predicted Dose Distribution (Predicted Output).

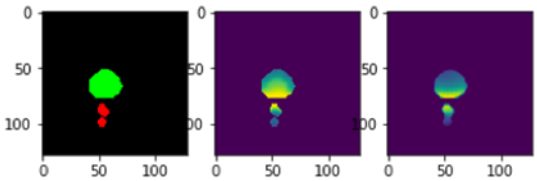

(B)Contoured Image (Input), Actual Dose Distribution (Expected Output), And Predicted Dose Distribution (Predicted Output).

Figure 6: Visualization Of The Input, Ground Truth, And Predicted Outputs For A Representative Mid-Slice From A Randomly Selected Patient's Ct Scan, Taken From The Validation Dataset. In This Illustration, The Bladder Is Highlighted Using The Green Channel, While The Rectum Is Represented In Red. The Color Intensity In The Middle And Right Columns Reflects The Percentage Of The Prescribed Radiation Dose Received By Each Voxel—Where Yellow Indicates A Higher Dose And Blue Corresponds To A Lower Dose.

VI. Result:

The Dose-Volume Histogram (DVH) and compared it with the DVHs derived from high-quality clinical treatment plans. As presented in Table VI and Figure 9, the performance of our model is on par with the results reported in knowledge-based planning approaches that utilize handcrafted features [18]. Notably, our model outperforms the prior work in most cases—specifically for bladder and all rectum cases except one in the V50%

category. For the volume percentages receiving at least 50% (V50%), 85% (V85%), and 99% (V99%) of the prescribed dose, our model demonstrates superior or equivalent performance. The Vx metric reflects the volume percentage that receives x% of the prescription dose. The relatively lower performance observed for the rectum at V50% may be attributed to the chosen slicing orientation. As discussed in Task 1, the axial view tends to lose more anatomical detail for the rectum compared to the sagittal view. Overall, based on numerical comparisons and patient-specific evaluations, our model consistently surpasses the previous study [18] for bladder predictions and shows competitive results for rectum cases. This is further illustrated in Figure 8, which compares predicted and actual DVHs for two randomly selected patients from the validation cohort, and in Figure 9, which highlights the performance across all patients for V50%, V85%, and V99%. These visualizations confirm a strong correlation between predicted and planned DVHs, aligning well with the findings illustrated in Figures 5 and 6 of the prior study [18]. Magnetic Resonance Imaging (MRI) offers superior soft tissue contrast without ionizing radiation, making it an ideal imaging modality for radiation therapy planning. Traditional radiotherapy workflows rely on computed tomography (CT) for dose calculation due to its accurate electron density information. However, integrating MRI alone into the dose estimation process presents an opportunity to reduce radiation exposure and streamline adaptive radiation therapy (ART). Deep learning plays a transformative role in this area by enabling synthetic CT (sCT) generation from MR images. These sCTs mimic CT-like images with electron density data, allowing accurate dose calculations directly from MRI inputs.

Deep learning models, particularly convolutional neural networks (CNNs) and generative adversarial networks (GANs), are trained on paired MR and CT datasets to learn complex image translation mappings. These models can produce highly realistic sCTs that support accurate dose distribution estimation. This MR-only approach enhances workflow efficiency, reduces image registration errors, and supports real-time adaptive treatment planning. Moreover, it enables continuous tracking of anatomical changes during treatment, improving precision and patient outcomes.

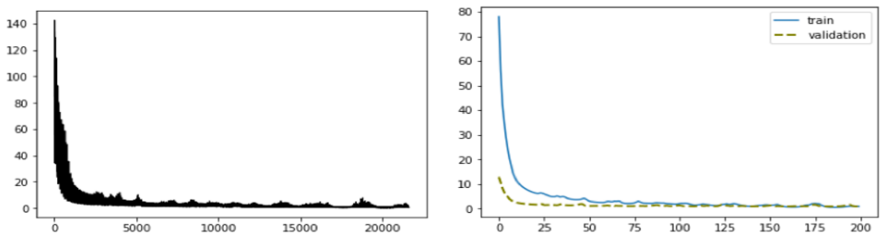

(A)Distance Representation **(B)Contour Representation**

Figure 7: To Perform A Comprehensive Patient-Level Evaluation And Facilitate A Direct Comparison

There are two primary strategies for feature extraction: one relies on domain expertise to design hand-crafted features, and the other allows machines to automatically learn patterns from diverse data points. While the latter approach—particularly through convolutional neural networks—has achieved remarkable success in fields like object classification, its effectiveness in healthcare remains limited. This is largely due to the scarcity of high-quality labeled datasets and the complexity of medical images, which involve a wide range of variables.

VII. Conclusion:

This study introduces and evaluates a hybrid approach that merges both human-guided and data-driven feature extraction methods for application in radiation therapy planning. Drawing inspiration from earlier research and expert insights, we replaced raw image data with distance matrices. This representation preserves the structural integrity of anatomical features while eliminating unnecessary intensity-based details.

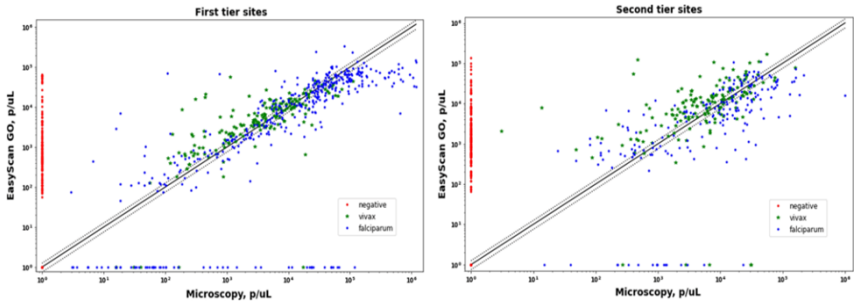

Figure 8: Comparison Of Predicted And Actual Dvh Curves For (A) Bladder And (B) Rectum, Highlighting The Predicted Volume At V99%, V85%, And V50%. The Error Bounds Corresponding To 6% And 10% Of The Oar (Organ At Risk) Volume Are Illustrated, Showing Comparability With Findings Reported In [18].

Our results show that this approach performs comparably to current state-of-the-art techniques, and it offers a promising direction for developing more generalizable and interpretable models in radiation therapy. The work advocates for further exploration into low-level feature engineering, effective use of pre-trained models, and thoughtful dimensionality reduction techniques to improve model performance and adaptability. Despite the encouraging outcomes, there is room for enhancement. For instance, in transfer learning scenarios, using more domain-relevant pre-trained models such as DeepLesion [17] could improve feature representation. Additionally, newer model architectures, like generative networks [9], should be considered for future evaluations. Beyond performance metrics, this feature representation offers practical benefits. It enables anonymization of CT data, facilitating safer and easier data sharing. As demonstrated in Task 1, it allows for independent analysis of each organ-at-risk (OAR) without the influence of other organs or the planning target volume (PTV), enhancing both prediction and learning. The representation's robustness to spatial displacements and orientation variations also introduces potential for effective data augmentation. Moreover, its interpretable structure creates opportunities for reverse engineering deep learning features—an essential step toward both validating model behavior and simplifying treatment planning through more intuitive formulations. [SELF]

Acknowledgment:

• **Corresponding Author:** Syed Anam Parvez from Teerthanker Mahaveer University, Moradabad, Uttar Pradesh, 244001.
• **Co- Author**: Ishant from Teerthanker Mahaveer University, Moradabad, Uttar Pradesh, 244001
• **Guidance**: Deepak Katiyar [ASSISTANT PROFESSOR] from Teerthanker Mahaveer University, Moradabad Uttar Pradesh,244001.

Abbreviation:

S.NO	ABBREVIATION	FULL FORM
1	2D	Two-Dimensional
2	3D	Three-Dimensional
3	ART	Adaptive Radiation Therapy
4	CGY	Centigray (Unit Of Radiation Dose)
5	CNN	Convolutional Neural Network
6	CT	Computed Tomography
7	DISTANCE3D	3d Distance Matrix Representation
8	DTH	Distance-To-Target Histogram
9	DVH	Dose-Volume Histogram
10	DVH3D	Three-Dimensional Dose-Volume Histogram
12	EBRT	External Beam Radiation Therapy
13	FCN	Fully Convolutional Network
14	IMRT	Intensity-Modulated Radiation Therapy
15	KBP	Knowledge-Based Planning
16	MR	Magnetic Resonance
17	NTCP	Normal Tissue Complication Probability
18	OAR	Organ-At-Risk
19	OVH	Overlap Volume Histogram
20	PTV	Planning Target Volume
21	QUANTEC	Quantitative Analysis of Normal Tissue Effects In The Clinic
22	U-NET	U-Shaped Convolutional Neural Network
23	VMAT	Volumetric Modulated Arc Therapy
24	VX	Volume Percentage Receiving At Least X% of The Prescribed Dose
25	V50%	Volume Receiving At Least 50% of The Prescription Dose

Reference:

[1] Ahunbay EE, Chen G-P, Thatcher S, Et Al. (2007). Direct Aperture Optimization–Based Intensity Modulated Radiotherapy For Whole Breast Irradiation. Int J Radiat Oncol Biol Phys, 67(4), 1248-1258.
[2] Arbea L, Ramos LI, Martínez-Monge R, Moreno M, Aristu J. (2010). Intensity-Modulated Radiation Therapy (IMRT) Vs. 3D Conformal Radiotherapy (3DCRT) In Locally Advanced Rectal Cancer (LARC): Dosimetric Comparison And Clinical Implications. Radiat Oncol, 5(1), 17.
[3] Armanious, K., Jiang, C., Fischer, M., Et Al. (2020). Medgan: Medical Image Translation Using Gans. Computerized Medical Imaging And Graphics, 79, 101684.
[4] Barkousaraie AS, Ogunmolu O, Jiang S, Nguyen D. (2019). A Fast Deep Learning Approach For Beam Orientation Optimization For Prostate Cancer IMRT Treatments. Arxiv Preprint Arxiv:190500523.
[5] Barragán-Montero AM, Nguyen D, Lu W, Et Al. (2019). Three-Dimensional Dose Prediction For Lung IMRT Patients With Deep Neural Networks: Robust Learning From Heterogeneous Beam Configurations. Med Phys.
[6] Bedford JL, Webb S. (2006). Constrained Segment Shapes In Direct-Aperture Optimization For Step-And-Shoot IMRT. Med Phys, 33(4), 944-958.
[7] Bortfeld T. (2006). IMRT: A Review And Preview. Phys Med Biol, 51(13), R363.
[8] Breedveld S, Craft D, Van Haveren R, Heijmen B. (2019). Multi-Criteria Optimization And Decision-Making In Radiotherapy. Eur J Oper Res, 277(1), 1-19.

[9] Breedveld S, Storchi PR, Voet PW, Heijmen BJ. (2012). Icycle: Integrated, Multicriterial Beam Angle, And Profile Optimization For Generation Of Coplanar And Noncoplanar IMRT Plans. Med Phys, 39(2), 951-963.
[10] Cassioli A, Unlatch J. (2012). Aperture Shape Optimization For IMRT Treatment Planning. Phys Med Biol, 58(2), 301.
[11] Chambolle A, Pock T. (2011). A First-Order Primal-Dual Algorithm For Convex Problems With Applications To Imaging. J Math Imaging Vis, 40(1), 120-145.
[12] Chang ATY, Hung AWM, Cheung FWK, Et Al. (2016). Comparison Of Planning Quality And Efficiency Between Conventional And Knowledge-Based Algorithms In Nasopharyngeal Cancer Patients Using Intensity Modulated Radiation Therapy. Int J Radiat Oncol Biol Phys, 95(3), 981-990.
[13] Chen X, Men K, Li Y, Yi J, Dai J. (2019). A Feasibility Study On An Automated Method To Generate Patient-Specific Dose Distributions For Radiotherapy Using Deep Learning. Med Phys, 46(1), 56-64.
[14] Convery D, Rosenbloom M. (1992). The Generation Of Intensity-Modulated Fields For Conformal Radiotherapy By Dynamic Collimation. Phys Med Biol, 37(6), 1359.
[15] Craft DL, Halabi TF, Shih HA, Bortfeld TR. (2006). Approximating Convex Pareto Surfaces In Multiobjective Radiotherapy Planning. Med Phys, 33(9), 3399-3407.
[16] Craft DL, Hong TS, Shih HA, Bortfeld TR. (2012). Improved Planning Time And Plan Quality Through Multicriteria Optimization For Intensity-Modulated Radiotherapy. Int J Radiat Oncol Biol Phys, 82(1), E83-E90.
[17] David EW, Marie D. (2001). A Call For Knowledge-Based Planning. AI Magazine, 22(1).
[18] Dinkla, A. M., Wolterink, J. M., Maspero, M., Et Al. (2019). MR-Only Brain Radiotherapy Using A Deep Learning Synthetic CT Generator. Radiotherapy And Oncology, 133, 204–208.
[19] Fan J, Wang J, Chen Z, Hu C, Zhang Z, Hu W. (2019). Automatic Treatment Planning Based On Three-Dimensional Dose Distribution Predicted From Deep Learning Technique. Med Phys, 46(1), 370-381.
[20] Fan J, Wang J, Zhang Z, Hu W. (2017). Iterative Dataset Optimization In Automated Planning: Implementation For Breast And Rectal Cancer Radiotherapy. Med Phys, 44(6), 2515-2531.
[21] Fenkell L, Kaminsky I, Breen S, Et Al. (2008). Dosimetric Comparison Of IMRT Vs. 3D Conformal Radiotherapy In The Treatment Of Cancer Of The Cervical Esophagus. Radiother Oncol, 89(3), 287-291.
[22] Fogliata A, Reggiori G, Stravato A, Et Al. (2017). Rapidplan Head And Neck Model: The Objectives And Possible Clinical Benefit. Radiat Oncol, 12(1), 73.
[23] Ge Y, Wu QJ. (2019). Knowledge-Based Planning For Intensity-Modulated Radiation Therapy: A Review Of Data-Driven Approaches. Med Phys, 46(6), 2760-2775.
[24] Gianfaldoni S, Gianfaldoni R, Wollina U, Et Al. (2017). An Overview On Radiotherapy: From Its History To Its Current Applications In Dermatology. Open Access Maced J Med Sci, 5(4), 521.
[25] Goodfellow, I., Bengio, Y., & Courville, A. (2016). Deep Learning. MIT Press.
[26] Greenspan H, Van Ginneken B, Summers RM. (2016). Guest Editorial Deep Learning In Medical Imaging: Overview And Future Promise Of An Exciting New Technique. IEEE Trans Med Imaging, 35(5), 1153-1159.
[27] Grégoire V, Mackie T. (2011). State Of The Art On Dose Prescription, Reporting And Recording In Intensity-Modulated Radiation Therapy (ICRU Report No. 83). Cancer/Radiothérapie, 15.
[28] Henke, L. E., Olsen, J. R., Contreras, J. A., Et Al. (2020). Adaptive MR-Guided Stereotactic Body Radiotherapy In The Treatment Of Oligometastatic Or Unresectable Primary Malignancies Of The Abdomen. Radiotherapy And Oncology, 145, 55–61.
[29] Hong T, Ritter M, Tomé WA, Harari P. (2005). Intensity-Modulated Radiation Therapy: Emerging Cancer Treatment Technology. Br J Cancer, 92(10), 1819.
[30] Jaffray, D. A., & Lindsay, P. E. (2009). Advances In Adaptive Radiation Therapy: Technological And Clinical Considerations. Journal Of Clinical Oncology, 27(26), 4111–4116.
[31] Jahn J. (1985). Scalarization In Multi Objective Optimization. In: Mathematics Of Multi Objective Optimization. Springer, 45-88.
[32] Jia X, Men C, Lou Y, Jiang SB. (2011). Beam Orientation Optimization For Intensity Modulated Radiation Therapy Using Adaptive L2,1-Minimization. Phys Med Biol, 56(19), 6205.
[33] Jiang, S. B., & Paganetti, H. (2019). Radiation Oncology Physics: A Handbook For Teachers And Students. CRC Press.
[34] Kajikawa T, Kadoya N, Ito K, Et Al. (2019). A Convolutional Neural Network Approach For IMRT Dose Distribution Prediction In Prostate Cancer Patients. J Radiat Res, 60(5), 685-693.
[35] Kearney V, Chan JW, Haaf S, Descovich M, Solberg TD. (2018). Dosenet: A Volumetric Dose Prediction Algorithm Using 3D Fully-Convolutional Neural Networks. Phys Med Biol, 63(23), 235022.
[36] Kingma D, Ba J. (2014). Adam: A Method For Stochastic Optimization. Arxiv Preprint Arxiv:14126980.
[37] Kristensen CA, Kjaer-Kristoffersen F, Sapru W, Et Al. (2007). Nasopharyngeal Carcinoma. Treatment Planning With IMRT And 3D Conformal Radiotherapy. Acta Oncol, 46(2), 214-220.
[38] Kubo K, Monzen H, Ishii K, Et Al. (2017). Dosimetric Comparison Of Rapidplan And Manually Optimized Plans In Volumetric Modulated Arc Therapy For Prostate Cancer. Phys Med, 44, 199-204.
[39] Lecun Y, Bengio Y, Hinton G. (2015). Deep Learning. Nature, 521(7553), 436–444.
[40] Lim, Y., Gao, Y., Et Al. (2021). Synthetic CT Generation And Its Applications In MR-Only Radiotherapy: A Review. Frontiers In Oncology, 11, 620038.
[41] Liu, Y., Lei, Y., Wang, T., Et Al. (2020). MRI-Based Treatment Planning For Radiation Therapy Using Deep Learning And Uncertainty Modeling. Medical Physics, 47(8), 3570–3581.
[42] Long J, Shelhamer E, Darrell T. (2015). Fully Convolutional Networks For Semantic Segmentation. Proc IEEE Conf Comput Vis Pattern Recognit.
[43] Lu W. (2010). A Non-Voxel-Based Broad-Beam (NVBB) Framework For IMRT Treatment Planning. Phys Med Biol, 55(23), 7175.
[44] Lu W, Chen M. (2010). Fluence-Convolution Broad-Beam (FCBB) Dose Calculation. Phys Med Biol, 55(23), 7211.
[45] Luxton G, Hancock SL, Boyer AL. (2004). Dosimetry And Radiobiologic Model Comparison Of IMRT And 3D Conformal Radiotherapy In Treatment Of Carcinoma Of The Prostate. Int J Radiat Oncol Biol Phys, 59(1), 267-284.